



New quartile-based region merging algorithm for unsupervised image segmentation using color-alone feature[☆]



Huang-Chia Shih*, En-Rui Liu

Human-Computer Interaction Multimedia Laboratory, Innovation Center for Big Data and Digital Convergence,
Department of Electrical Engineering, Yuan Ze University, Taoyuan, Taiwan, ROC

ARTICLE INFO

Article history:

Received 13 October 2014

Revised 25 November 2015

Accepted 26 December 2015

Available online 4 January 2016

Keywords:

Color vector ordering

Image segmentation

Mathematical morphology process

Quartile analysis

Reference color selection

Region merging

ABSTRACT

This study concerns the image segmentation problem and the use of a color-alone feature for reducing the system complexity. On the basis of the color-based mathematical morphology method, the similarity measure between neighboring regions can be obtained as the solution of a ranking problem. To avoid the creation of a false color and false segmentation, a hybrid ordering approach was used instead of vectorized and marginal ordering approaches. Ordering methods that use black as the reference color to sort pixels face a problem: the scope of distance measurement is not optimal. To avoid this problem, we present a scheme for selecting a global reference color. Moreover, for determining orders of color vectors, the hue-saturation-intensity color distance was used instead of the Euclidean distance. The aforementioned scheme involves segmentation that is in accord with human visual perception. Quartile analysis indicated that threshold determination for region-merging showed less sensitivity to context variations of images. To evaluate the algorithm, it was experimentally compared with two typical segmentation schemes on the basis of four quantitative indices.

© 2016 Published by Elsevier Inc.

1. Introduction

Image segmentation is one of the most critical topics related to computer vision applications [39,41,51,53,62], and numerous segmentation methods based on primary image features such as color and texture have been proposed. Over the past decade, algorithms for integrating color and texture descriptors have attracted considerable attention; for example, a model-based energy function [28], graph-based representation [19], a Gaussian mixture model [40], a Markov random field [16], ensemble clustering [30], constrained Laplacian optimization [49], fuzzy labeling [10], and some well-known algorithms involving implicit integration of color and texture features, such as J -mage-based segmentation [15], Gibbs random fields [46], CTex [25], gradient-based segmentation [55], and normalized cuts [50], have been developed. Additional information on color-texture descriptors can be found in reviews [26]. Nevertheless, to achieve a trade-off between segmentation accuracy and computational cost, many studies have considered color-alone [1,43,48] and texture-alone [35,45,54] image information. Region-based approaches that treat color and texture features separately have arguably been the most investigated segmentation schemes. These types of approaches are based on the consistency of the spatial coherence between adjacent pixels.

[☆] The work reported in this paper was partially published in the 12th *Asian Conference on Computer Vision (ACCV '14)*.

* Corresponding author. Tel.: +886 3 463 8800; fax: +886 463 9355.

E-mail address: hcsih@saturn.yzu.edu.tw (H.-C. Shih).

Split and merge techniques enable the segmentation process to be hierarchically analyzed at different levels: pixel, region, object, and semantic levels.

In recent years, because of the advantages of using set theory in image processing, mathematical morphology (MM) [4,6,9] has been widely used in image processing; for example, it has been used for image retrieval [7], satellite imagery analysis [44], galaxy classification [5], and image segmentation [38,47,61]. MM can easily be applied to high-dimensional image data, from binary and grayscale images to color images and even higher dimensions of visual features [14,22]. This is crucial for the continual development of image processing, which tends to consider only the illumination information of pixels. However, the use of MM typically involves neglecting the minutiae of the image content. In view of continuing advances in color image acquisition techniques, their compatibility with extant algorithms should be extended, and must be as concrete as possible. An MM process is based on lattice theory of a spatial structure [3]. Therefore, understanding the relationship between pixels and sorting them according to their characteristics is crucial. However, ranking higher-dimensional vectors in a straightforward manner is difficult, and modeling the geometry of a vector-valued function is of little value. Unlike single-dimensional images (e.g., binary and grayscale images), there is no standard ordering mechanism for color feature vectors.

Generally, approaches used for color ordering for color morphological processing can be divided into two categories: marginal-oriented and vector-oriented approaches. In the marginal-oriented approach (i.e., M-ordering) [63], each color component is independently considered. In other words, the marginal correlation between color components is ignored and each color component is considered as a grayscale image. By contrast, in the vector-oriented approach, color morphological process is performed using a vectorized ordering method, such as reduced ordering (i.e., R-ordering) [33,57], conditional ordering (i.e., C-ordering) [8], and partial ordering (i.e., P-ordering) [17,18].

Some studies have presented methods, other than those involving the aforementioned four ordering methods, from a different viewpoint. For example, Lezoray et al. [29] presented a graph-based ordering method in which the structural element was considered as a complete graph and each vertex in the graph represented an image pixel. A weighted factor was assigned to each of the edges in the graph, and the minimum spanning tree method was then used to rank the elements of a vector. Furthermore, other studies [2,21,32,60] have presented composite ranking methods, including R + C ordering, P + M ordering, and bit-mixing ordering for the MM processing of color images.

In the present study, we employed the color ordering method presented in our previous study [52], called color-based reduced and conditional (CRC) ordering. Other Euclidean-distance-based ordering methods in which black is used as the reference color for sorting pixels [59] pose a problem: the scope of distance measurement is not optimal. Therefore, we present a scheme in which a global reference color can be selected through hue–saturation–intensity (HSI) distance measurement. This scheme helps deal with diverse color models and avoids the ambiguous situation associated with ranking comparisons of color vectors. Finally, we propose an adaptive merging algorithm that does not require threshold determination. We present a novel automatic threshold determination method, which involves quartile analysis, for use in the region merging process. This approach rendered region merging simpler and more practical.

The main contribution of this study is the presentation of an image segmentation method based on a color-alone feature and involving low system complexity is presented. Observations showed that the morphological ordering efficiency is strongly dependent on the image color distribution. We adopted the color complementary to the dominant color of the test region as the reference color. Moreover, the HSI color distance was used instead of the Euclidean distance for determining orders of color vectors. The result of the proposed methods is in accord with subjective human perception, especially in regions with small patches. Furthermore, oversegmentation is rare, unlike other watershed-based image segmentation methods. Quartile analysis has shown that threshold determination is less sensitive to context variations of the test image. The burden of threshold determination is avoided substantially, enabling an authentic segmentation result to be achieved. Such segmentation renders region merging simple, practical, and appropriate for large data applications [12,34].

The remaining part of this paper is organized as follows. Section 2 presents the proposed color ordering scheme for color-based MM. Section 3 details the image segmentation algorithm, including pre-segmentation, region merging through hybrid ordering, and adaptive threshold determination. Experimental results are presented in Section 4. Finally, we discuss our findings and draw conclusions in Section 5.

2. Color ordering scheme

2.1. Global reference color selection

In the literature, available information on the selection of the global reference color c_{ref}^g is scant. Generally, the main criterion for color selection is to select the pixel that is the most distinct from the test color pixel. Many studies [2,3,29] have used black as the reference color. However, this creates a problem: the scope of distance measurement is not optimal. In other words, the ordering efficiency is highly dependent on the image color distribution. To overcome this problem, we must consider the image color distribution for obtaining the dominant color. The most appropriate reference color is the color complementary to the dominant color. This method evidently yields the distance measure for achieving the highest discriminative ability. Nevertheless, when the dominant color is located in the spatial information plane, such as $(1/2, 1/2,$

1/2) in a normalized space of colors, we simply consider black as the reference color. Details of the reference color selection method are provided in a previously published paper [52].

2.2. Hybrid ordering algorithm

We propose a hybrid color ordering method that involves CRC ordering. Apart from retaining the advantages of R-ordering (i.e., reducing the dimension of the feature vector and thereby decreasing the computational cost), this method avoids the ambiguous situation created by C-ordering during the measurement of the importance of the color vector. The CRC ordering approach is illustrated by using three phases as follows:

2.2.1. Global ranking

R-ordering is a color ranking operation that is based on the distance between the test pixel color and the reference color projected onto the color space:

$$c_p <_{c_{ref}^g} c_q \Leftrightarrow \|c_p - c_{ref}^g\|_{d_{HSI}}^{HSI} > \|c_q - c_{ref}^g\|_{d_{HSI}}^{HSI}, \quad (1)$$

where c_p and c_q denote pixels with different color components, “ \Leftrightarrow ” denotes an “if and only if” relationship, $<_{c_{ref}^g}$ denotes the pixel-based comparison operator for the selected global reference color c_{ref}^g , $\|\cdot\|_{d_{HSI}}^{HSI}$ denotes the measured HSI distance d_{HSI} , and the superscript “HSI” indicates that the HSI color model was used.

2.2.2. Local ranking

C-ordering was used for avoiding an ambiguous situation. For example, if there are two color pixels with different color components but at the same distance from the reference pixel in color space, then they are classified as having the same color. To avoid this situation, the C-ordering method is used in the proposed CRC ordering algorithm. This method is also called lexicographical ordering and can be expressed as

$$c_p <_{CRC} c_q \Leftrightarrow \left\{ \begin{array}{l} \|c_p - c_{ref}^g\|_{d_{HSI}}^{HSI} > \|c_q - c_{ref}^g\|_{d_{HSI}}^{HSI} \quad \text{or} \\ \|c_p - c_{ref}^g\|_{d_{HSI}}^{HSI} \leq \|c_q - c_{ref}^g\|_{d_{HSI}}^{HSI} \quad \text{and} \\ \left\{ \begin{array}{l} c_p^I < c_q^I \quad \text{or} \\ c_p^I = c_q^I \quad \text{and} \quad c_p^S < c_q^S \quad \text{or} \\ c_p^I = c_q^I \quad \text{and} \quad c_p^S = c_q^S \quad \text{and} \quad c_p^H < c_q^H \end{array} \right. \end{array} \right. , \quad (2)$$

where $c_p = (c_p^H, c_p^S, c_p^I)$ and $c_q = (c_q^H, c_q^S, c_q^I)$ represent two pixels and contain the HSI color information of the pixels.

The main task in the C-ordering method is to sort each color component with a particular ordering priority. An appropriate ordering priority depends on the context of the images. The consideration of the priority helps the system obtain different morphological processing results by adjusting the order of comparisons among the color components. For example, when dilation operation is performed in the RGB color space with the priority $R \rightarrow G \rightarrow B$, the red color tone of the test image is enhanced considerably. Conversely, when the priority $G \rightarrow R \rightarrow B$ is adopted, the green color tone is enhanced. However, human eyes are very sensitive to RGB color space, and if the color values are processed in the conventional manner, it results in an unreal and false color appearance. The HSI color model is based on human perception of color, and it is frequently adopted for image processing. In edge detection applications, the priority $I \rightarrow S \rightarrow H$ is more appropriate than $H \rightarrow S \rightarrow I$ because the boundary of an object shows a sharp intensity change. In addition, the human eye is sensitive to minor changes in the intensity but not in color. If we consider that the color component is more important than intensity (for example, for skin color tone detection), then to suppress distortions produced by the flickering of the light source, the morphological operator can be employed with the priority $H \rightarrow S \rightarrow I$. With this priority, the brightness sensitivity need not be increased in applications of color-based image processing.

3. Image segmentation based on hybrid ordering and quartile analysis

The bottom-up image segmentation method comprises three parts: (i) watershed pre-segmentation based on a color gradient image, (ii) region merging by using hybrid ordering, and (iii) adaptive threshold determination by using quartile analysis. To obtain a color gradient image by using CRC-ordering-based MM, we first performed watershed image segmentation to roughly segment the original image. On the basis of region distance, we then used a sequential region merging scheme for segmenting the image. Finally, we used the quartile analysis method for determining the best threshold for merging adjacent regions.

3.1. Image pre-segmentation

The purpose of this phase is to extract the initial partitions of the image by adopting a color gradient and through watershed-based segmentation. Watershed-based segmentation, first presented by Vincent and Soille [58], is one of the most efficient image segmentation methods. A major feature of this method is the consideration of the original image as a stereo mountain diagram. The gradient energy is considered to be represented by the rise and fall of the mountain.

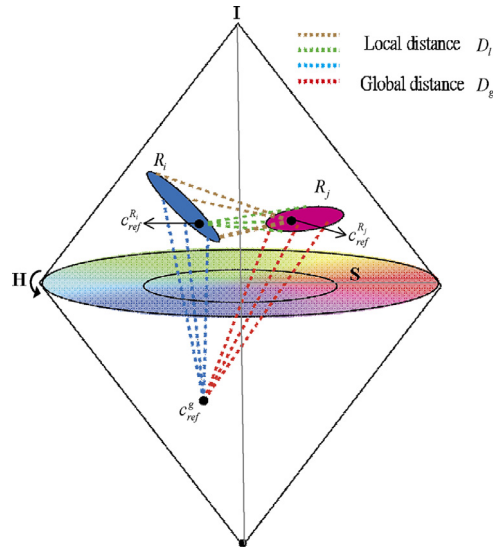


Fig. 1. Distance measurement in global and local viewpoints. (For interpretation of the references to color in this figure legend, the reader is referred to the web version of this article.)

3.2. Region merging through hybrid ordering

The traditional watershed method has the disadvantage of over segmenting a small region because of noise and specific image patterns, resulting in the image segmentation performance being considerably degraded. Hence, we propose a more robust region merging algorithm. In addition, on the basis of the concept of distance, region-based MM was used to determine the likelihood of two adjacent regions being merged.

Suppose that a region is initially partitioned through watershed segmentation and that the partitions are denoted by $S = (R_1, \dots, R_n)$. The objective of image merging is to obtain a merger discrimination matrix P that represents the final segmentation. We then tag the watershed image as the initial image and perform the merging step using the bottom-up scenario. The merging step involves a global search for the two tags (i.e., regions) with the minimum difference. This difference refers to the mean of the color distance D_g derived from the reference color, which uses the dominant color of the entire image (i.e., global rank), which are depicted by the red and blue dashed lines in Fig. 1. If we assume that $R_i = (p_1, \dots, p_n)$ and $R_j = (q_1, \dots, q_m)$ represent two groups of pixels in adjacent regions, the global distance of R_i can be computed as

$$D_g(R_i, c_{ref}^g) = \frac{1}{n} \sum_{k=1}^n d_{HSI}(p_k, c_{ref}^g), \tag{3}$$

where d_{HSI} is the HSI distance and c_{ref}^g denotes the global reference color. According to Eq. (3), the ranking relationship between the two regions corresponding to these average color distances can be determined through R-ordering:

$$R_i <_{c_{ref}^g} R_j \Leftrightarrow D_g(R_i, c_{ref}^g) > D_g(R_j, c_{ref}^g). \tag{4}$$

To prevent the creation of an ambiguous situation, we used the C-ordering scheme in the proposed segmentation method. From a local viewpoint, we computed the difference value D_l between the two adjacent regions. More specifically, we measured the average color distance by using the dominant color as the reference color in the HSI color space, indicated by the dotted brown and green dashed lines shown in Fig. 1. The average color distance is defined as

$$D_l(R_i, c_{ref}^{R_j}) = \frac{1}{n} \sum_{k=1}^n d_{HSI}(p_k, c_{ref}^{R_j}), \tag{5}$$

where $c_{ref}^{R_j}$ denotes the reference color for region R_j .

From Eqs. (4) and (5), the CRC ordering operation $<_{CRC}^R$ can be expressed as

$$R_i <_{CRC}^R R_j \Leftrightarrow \begin{cases} D_g(R_i, c_{ref}^g) > D_g(R_j, c_{ref}^g) & \text{or} \\ D_g(R_i, c_{ref}^g) \leq D_g(R_j, c_{ref}^g) & \text{and} \\ \left\{ D_l(R_i, c_{ref}^{R_j}) < D_l(R_j, c_{ref}^{R_i}) \right\}. \end{cases} \tag{6}$$

Algorithm 1
CRC-ordering region merging

Estimation of the merge relationship between two regions

1. **Initialization:** Apply the watershed segmentation, $S = (R_1, \dots, R_n)$.
2. **Input** $S = (R_1, \dots, R_n)$
3. Choose the reference color globally c_{ref}^g ;
4. **Repeat**
5. Process R_i and R_j based on CRC-ordering $<_{CRC}^R$;
6. Find $D_g(R_i, c_{ref}^g)$ and $D_g(R_j, c_{ref}^g)$ for R_i and R_j respectively;
7. **If** $|D_g(R_i, c_{ref}^g) - D_g(R_j, c_{ref}^g)| < TH_g$ **then**
8. Compute $D_l(R_i, c_{ref}^g)$ and run $R_i <_{CRC}^R R_j$;
9. **If** $D_l(R_i, R_j) < TH_l$ **then** $P(R_i, R_j) = \text{true}$;
10. Merged R_i and R_j ;
11. **End if**
12. **End if**
13. **Update region information**
14. **Until convergence**
15. **Output** segmentation S

The merger discrimination matrix P can then be constructed using the global threshold TH_g and local threshold TH_l :

$$P(R_i, R_j) = \begin{cases} \text{true if } D_g(R_i, R_j) < TH_g \text{ and } D_l(R_i, R_j) < TH_l \\ \text{false otherwise.} \end{cases} \quad (7)$$

Empirically, TH_g can be adjusted by varying the color distribution entropy, and TH_l depends on the local probability density over the entire image. Finally, CRC ordering is achieved by determining the minimum difference value. When $D_g(R_i, R_j)$ is less than TH_g and $D_l(R_i, R_j)$ is less than TH_l , the two regions can be merged. The algorithm is terminated when this difference value is greater than a predefined threshold. This segmentation procedure is shown as Algorithm 1.

As mentioned, the proposed ordering method is required to determine a threshold value for managing region merging. For different images, a specific threshold is required. The system has limitations and is not practical because obtaining a generic threshold is a challenging task. Consequently, we propose a merging algorithm that does not require threshold determination. This simplifies the region merging process and makes it more flexible. In the following section, we introduce a quartile-analysis-based robust automatic threshold determination method for merging regions. To demonstrate the feasibility of this method, we present a comparison of the performance of this method with that of CRC ordering (Algorithm 1) in the experimental section.

3.3. Adaptive threshold determination

As mentioned, in the CRC ordering method, a threshold value should be determined for performing region merging. For different images, a specific threshold is required. To obtain the threshold, we performed quartile analysis for adjacent regions and determined the best threshold for merging them.

3.3.1. Quartile analysis

Quartile analysis is a statistical method [24,27]. The quartiles of a ranked set of values are the three points that divide the data set into four equal groups. Therefore, each group comprises a quarter of the data. The values of the three points are 25%, 50%, and 75% of the highest value of the data set, and the points with these values are denoted by Q_1 , Q_2 , and Q_3 , respectively. Furthermore, the value of $Q_1 - Q_3$ is called interquartile range (IQR), and it is typically used to characterize data in the presence of extremities that skew the data. The IQR is a relatively robust statistic compared with the range and standard deviation, and it represents the distribution among 50% of data set approaching to the median value. Quartiles along with the upper and lower limits of the data set can be used to ascertain the existence of outliers and to determine “fences”. A data point is called an outlier when it lies outside the range $[Q_1 - k(Q_3 - Q_1), Q_3 + k(Q_3 - Q_1)]$, where k denotes a non-negative constant.

3.3.2. Region merging algorithm involving quartile analysis

On the basis of the quartiles Q_1 and Q_3 , we analyzed the distributions of two neighboring regions R_i and R_j . The values of the HSI color distance from the reference color c_{ref}^g were considered as the data set for the quartile analysis, and the values of Q_1 , Q_2 , and Q_3 were obtained. Finally, the IQR was used to determine whether R_i and R_j were to be merged. Suppose that the number of pixels in R_i is greater than that in R_j . As shown in Fig. 2, there are four possible cases in the quartile analysis:

- (1) First case: The HSI distance distribution of R_j is completely included in R_i . Therefore, we have $Q_1^g(R_j, c_{ref}^g) > Q_1^g(R_i, c_{ref}^g)$ and $Q_3^g(R_j, c_{ref}^g) < Q_3^g(R_i, c_{ref}^g)$. These relations indicate that the color distribution of R_j belongs to R_i too. In this case, regions R_j and R_i are allowed to merge and assigned the highest priority for merging.

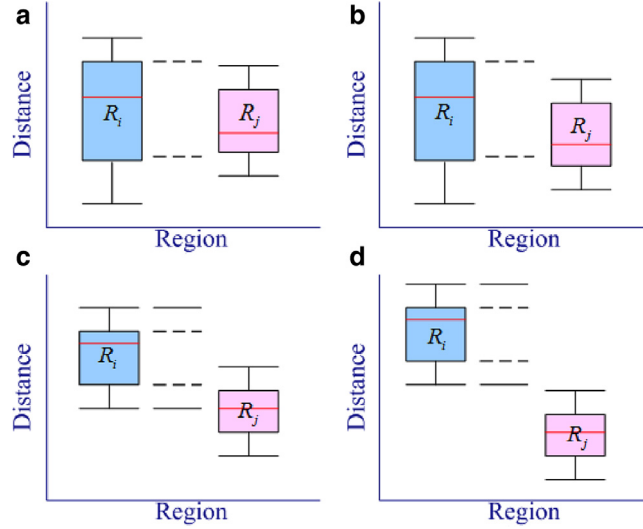


Fig. 2. Quartile analysis to four cases for merge determination, (a) first priority to merge, (b) second priority to merge, (c) third priority to merge, (d) do not merge.

(2) Second case: The HSI distance distribution of R_j is partially included in R_i , and we have

- (a) $Q_1^g(R_j, c_{ref}^g) > Q_1^g(R_i, c_{ref}^g)$ and $Q_1^g(R_j, c_{ref}^g) < Q_3^g(R_i, c_{ref}^g)$ or
 (b) $Q_3^g(R_j, c_{ref}^g) > Q_1^g(R_i, c_{ref}^g)$ and $Q_3^g(R_j, c_{ref}^g) < Q_3^g(R_i, c_{ref}^g)$.

These relations show that part of the color distribution of R_j is included in R_i . In this case, regions R_j and R_i are allowed to merge and the second highest priority is assigned.

(3) Third case: The HSI distance distribution of R_j is absent in R_i . However, the distribution range of R_j continues to lie within the maximum and the minimum observed values of R_i (i.e., 1.5 times the IQR), and it satisfies the following conditions:

- (a) $Q_1^g(R_j, c_{ref}^g) > Q_{1-1.5IQR}^g(R_i, c_{ref}^g)$
 (b) $Q_1^g(R_j, c_{ref}^g) < Q_{3+1.5IQR}^g(R_i, c_{ref}^g)$
 (c) $Q_3^g(R_j, c_{ref}^g) > Q_{1-1.5IQR}^g(R_i, c_{ref}^g)$
 (d) $Q_3^g(R_j, c_{ref}^g) < Q_{3+1.5IQR}^g(R_i, c_{ref}^g)$

These relations indicate that the color distribution of R_j is not present in R_i . However, it remains within the tolerance range for R_i . In this case, R_j and R_i are permitted to merge and are assigned the third highest priority.

(4) Fourth case: The HSI distance distribution range of R_j is completely included in R_i , but lies outside the maximum and minimum observation values of R_i (i.e., 1.5 times the IQR). This indicates that the pixels in R_j and R_i are completely different. Hence, the two regions cannot be merged in this case.

By considering the aforementioned four cases and priorities, we used the bottom-up scenario to merge a region with less pixels into another region with more pixels until convergence. We computed the color distance between each segmented region and the global reference color c_{ref}^g to determine the merging priority. To ensure accurate merging, we considered the local properties of the image. By examining whether the local color distance between adjacent regions exceeds 1.5 times the IQR of the observation range, we can avoid ambiguous situations associated with the use of only the global distance measure. In summary, we performed quartile analysis to understand data distributions. The pseudo-code of the quartile-based region merging algorithm is shown in [Algorithm 2](#).

4. Experimental results

To evaluate the performance of the proposed method, we used a personal computer with a 2.66 GHz Intel® Core™ i5-750 CPU and 4 GB main memory. The software used was Dev-C/C++ 4.9.9.2 and MATLAB 7.11.0, and the test images were obtained from the Berkeley Segmentation Dataset [11].

We compared the results of the proposed CRC ordering scheme with those of other typical schemes used in image segmentation, including the marker-controlled watershed method [42] and the mean shift clustering method [13]. We considered four standard indices to quantitatively evaluate the performance of our proposed method.

Algorithm 2
Quartile-based region merging

Estimation of the merge relationship between two regions

1. **Initialization:** Apply the region segmentation, $S = (R_1, \dots, R_n)$.
 2. **Input** $S = (R_1, \dots, R_n)$
 3. Choose the reference color globally c_{ref}^g ;
 4. **Repeat**
 5. Find $Q_1^g(R_i, c_{ref}^g)$ and $Q_2^g(R_j, c_{ref}^g)$ for R_i and R_j respectively and $V_{R_i} > V_{R_j}$;
 6. **If** $Q_1^g(R_j, c_{ref}^g) > Q_1^g(R_i, c_{ref}^g)$ and $Q_2^g(R_j, c_{ref}^g) < Q_2^g(R_i, c_{ref}^g)$ **then**
 7. **If** $Q_2^l(R_j, c_{ref}^{R_i}) < Q_{1-1.5IQR}^l(R_j, c_{ref}^{R_i})$ and $Q_2^l(R_j, c_{ref}^{R_i}) < Q_{3+1.5IQR}^l(R_j, c_{ref}^{R_i})$ **then**
 8. Merged R_j to R_i
 9. **Else if** $\{Q_1^g(R_j, c_{ref}^g) > Q_1^g(R_i, c_{ref}^g)$ and $Q_1^g(R_j, c_{ref}^g) < Q_3^g(R_i, c_{ref}^g)\}$ or $\{Q_3^g(R_j, c_{ref}^g) > Q_3^g(R_i, c_{ref}^g)$ and $Q_3^g(R_j, c_{ref}^g) < Q_1^g(R_i, c_{ref}^g)\}$ **then**
 10. **If** $Q_2^l(R_j, c_{ref}^{R_i}) < Q_{1-1.5IQR}^l(R_j, c_{ref}^{R_i})$ and $Q_2^l(R_j, c_{ref}^{R_i}) < Q_{3+1.5IQR}^l(R_j, c_{ref}^{R_i})$ **then**
 11. Merged R_j to R_i
 12. **Else if** $\{Q_2^g(R_j, c_{ref}^g) > Q_{1-1.5IQR}^g(R_i, c_{ref}^g)$ and $Q_2^g(R_j, c_{ref}^g) < Q_{3+1.5IQR}^g(R_i, c_{ref}^g)\}$ and $\{Q_3^g(R_j, c_{ref}^g) > Q_{1-1.5IQR}^g(R_i, c_{ref}^g)$ and $Q_3^g(R_j, c_{ref}^g) < Q_{3+1.5IQR}^g(R_i, c_{ref}^g)\}$ **then**
 13. **If** $Q_2^l(R_j, c_{ref}^{R_i}) < Q_{1-1.5IQR}^l(R_j, c_{ref}^{R_i})$ and $Q_2^l(R_j, c_{ref}^{R_i}) < Q_{3+1.5IQR}^l(R_j, c_{ref}^{R_i})$ **then**
 14. Merged R_j to R_i ;
 15. **End if**
 16. **Update region information**
 17. **Until convergence**
 18. **Output** segmentation S
-

4.1. Measures of objective evaluation

In this study, four indices were used to quantitatively compare typical methods.

4.1.1. Normalized probabilistic random index [56]

The probabilistic random index (PRI) can be used to evaluate the segmentation performance with respect to a ground truth image. The normalized probabilistic random index (NPRI) is an extension of the PRI, and it facilitates meaningful comparison of scores between segmented and ground truth images. Assume that an n -pixel image is to be segmented, and let S_g and S_t denote a manual partition of the ground truth image and an actual partition of the test image, respectively. Assume that there are n nonoverlapping regions in $S_g: \{R_1^g, R_2^g, \dots, R_n^g\}$ and n' regions in $S_t: \{R_1^t, R_2^t, \dots, R_{n'}^t\}$. For an explicit and quantitative evaluation of image segmentation, it is necessary that for any given pair of pixels (x_i, x_j) , the obtained labels l_i and l_j in S_g should be fully consistent with the labels l'_i and l'_j in S_t . Therefore, we have

$$PRI(S_g, S_t) = \frac{1}{c_n^2} \sum_i \sum_{j(i \neq j)} [\mathbf{I}(l_i = l_j \text{ and } l'_i = l'_j) + \mathbf{I}(l_i \neq l_j \text{ and } l'_i \neq l'_j)], \quad (8)$$

where \mathbf{I} denotes a discriminant function. The NPRI reflects the amount of variance inherent in the test data set and is given by following equation:

$$NPRI(S_g, S_t) = \frac{PRI(S_g, S_t) - \text{Expected index}}{\text{Maximum index} - \text{Expected index}}. \quad (9)$$

4.1.2. Variation of information [37]

Variation of information (Vol) is based on the relationship between a pixel and its cluster, and it is used for determining the distance between a certain segment and another segment by using a common information metric and the conditional entropy. Assume that image S , where $S = \cup_{k=1}^K S_k$, is partitioned into K segments. If the number of pixels in the k th region S_k is n_k , then the associated probability is $P(k) = n_k/n$. Hence, the entropy of the segmented image S can be computed as

$$H(S) = - \sum_{k=1}^K P(k) \log P(k). \quad (10)$$

Consider a $K \times K'$ parallel matrix denoted by $N = [n_{kk'} | k = 1, 2, \dots, K; k' = 1, 2, \dots, K']$. This matrix is used to indicate the relationship between clusters of S_g and S_t . Each component $n_{kk'}$ denotes the intersection of pixels of S_g and S_t . For any pixel in S_g that has been classified as belonging to the k th cluster (denoted as S_k^g), the pixel in S_t with which it intersects is classified as belonging to the k' th cluster in S_t (i.e., $S_{k'}^t$), and the joint probability of this condition can be expressed as

$$I(S_g, S_t) = \sum_{k=1}^K \sum_{k'=1}^{K'} P(k, k') \log \left[\frac{P(k, k')}{P(k)P(k')} \right]. \quad (11)$$

The definition of Vol involves the combination of the entropies of the ground truth image and the actual segmented image and the joint probability between them:

$$\text{Vol}(S_g, S_t) = H(S_g) + H(S_t) - 2I(S_g, S_t). \tag{12}$$

Vol has been used to measure the difference in information between the segmented image and the ground truth image. The smaller the value of Vol, the lesser the difference. In other words, Vol indicates how close the actual segmented result is to the reference ground truth image.

4.1.3. Global consistency error [36]

The global consistency error (GCE) is an error measure that quantifies the consistency between image segmentation results. This index gives the probability of any two partitions being classified as belonging to the same subimage on different scales. For a given pixel of the test image, p_i , the p_i -containing classes (segments) in the ground truth image (i.e., $p_i \in S_k^g$) and in actual segmented images are considered, where $p_i \in S_{k'}^t$. If $S_k^t \in S_{k'}^g$, then the local refinement error can be written as

$$E(S_k^g, S_{k'}^t, p_i) = R(S_k, p_i) \setminus R(S_{k'}^t, p_i) / R(S_k^g, p_i), \tag{13}$$

where $R(\cdot)$ denotes the collection of pixels in the corresponding class and the symbol “\” denotes set difference.

This error measure is not symmetric and encodes the local refinements in one direction only; in other words, $E(S_k^g, S_{k'}^t, p_i) \neq E(S_{k'}^t, S_k^g, p_i)$. If the segment S_k^g is a subset of the segment $S_{k'}^t$, then the pixel p_i in $S_{k'}^t$ does not with local error, that is, $E(S_k^g, S_{k'}^t, p_i) = 0$; otherwise, if the segments S_k^g and $S_{k'}^t$ do not have a subset relationship, then the areas where these two individual segments overlap are not continuous, that is, $E(S_k^g, S_{k'}^t, p_i) \neq 0$.

The GCE forces all local refinements to have the same direction, and it can be expressed as follows:

$$\text{GCE}(S_g, S_t) = \frac{1}{n} \min \left\{ \sum_i E(S_g, S_t, p_i), \sum_i E(S_t, S_g, p_i) \right\}. \tag{14}$$

If the value of the GCE is small, it indicates a small image segmentation error.

4.1.4. Boundary displacement error [20]

The boundary displacement error (BDE) represents the average offset error of a boundary pixel between two segmented regions. It defines the error in the distance between a certain pixel on the boundary and the closest boundary pixel in another segment. Let S_t and S_g denote two segments, as defined before. For a given pixel p_i in S_t , the minimum Euclidean distance (MED) from p_i to all pixels in S_g is calculated. The distance distribution signature $D_{S_t}^{S_g}$ store all MEDs among pixels in S_t and S_g . Finally, we can obtain the BDE by using the expression

$$\text{BDE}(S_t, S_g) = \frac{1}{2} (D_{S_t}^{S_g} + D_{S_g}^{S_t}). \tag{15}$$

4.2. Comparison of the proposed segmentation method with typical methods

First, two state-of-the-art segmentation methods were used in the evaluation of the system. Table 1 shows a quantitative comparison of the methods. Empirically, the unified merger threshold TH_l of 0.65 is considered. We tested 300 images from the Berkeley Segmentation Dataset [11]. In Table 1, Rank 1 denotes the segmentation results ranked first, and Rank 2 denotes the median rank. On the basis of the results of the quantitative evaluation shown in Table 1, the proposed CRC ordering algorithm outperforms other algorithms in evaluating the NPRI, Vol, and the BDE. However, the evaluation with

Table 1
Comparison of different image segmentation algorithms.

Algorithms	Performance evaluations							
	NPRI [56]		Vol [37]		GCE [36]		BDE [20]	
	Rank1	Rank2	Rank1	Rank2	Rank1	Rank2	Rank1	Rank2
CRC-ordering	120(40.0%)	279(93.0%)	96(32.0%)	285(95.0%)	12(4.0%)	91(30.3%)	119(39.7%)	293(97.7%)
Maker watershed [42]	14(4.7%)	43(14.3%)	189(63.0%)	263(87.7%)	214(71.3%)	257(85.7%)	6(2.0%)	12(4.0%)
Mean-shift clustering [13]	166(55.3%)	278(92.7%)	15(5.0%)	52(17.3%)	74(24.7%)	252(84.0%)	175(58.3%)	295(98.3%)
Algorithms	Performance evaluations over the Berkeley Segmentation Database							
	NPRI [56]	Vol [37]	GCE [36]	BDE [20]				
SAS [31]	0.8319	1.6849	0.1779	11.29				
SLIC superpixels [23]	0.8474	1.5542	N/A	11.15				
Ours	0.8587	1.5947	0.1968	11.19				

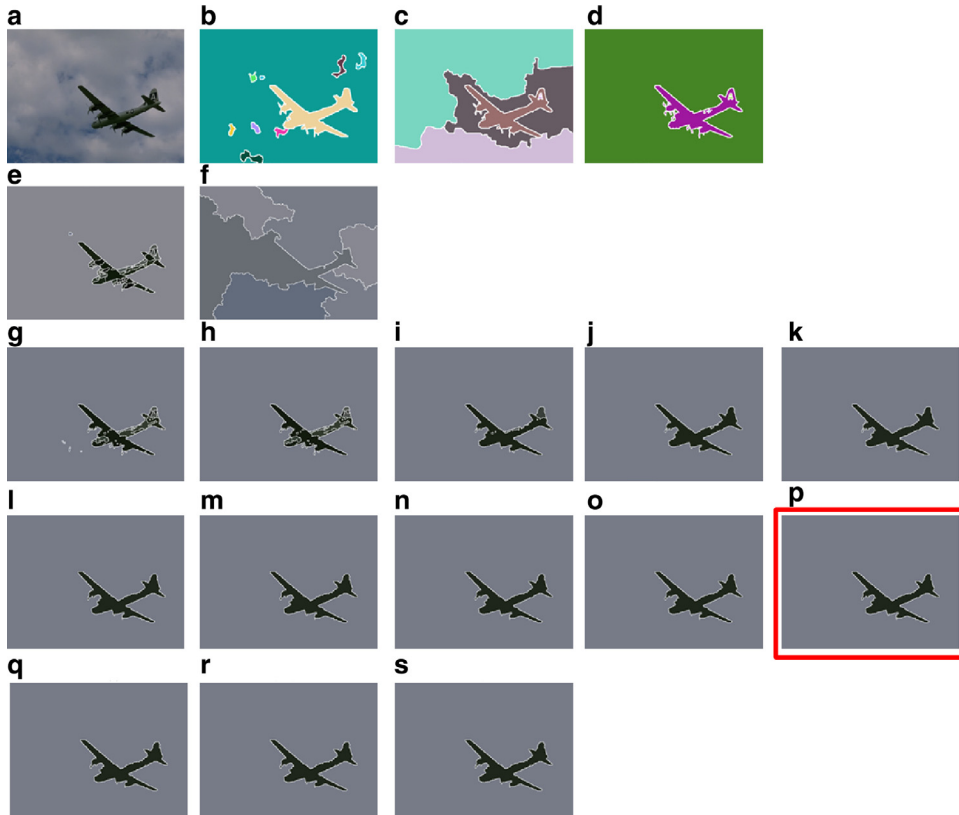


Fig. 3. Image segmentation results: airplane. (a) Original image, (b)–(d) ground-truth boundary, (e) mean-shift clustering method, (f) marker watershed method, (g)–(s) CRC-ordering result for different thresholds (i.e., $TH_i = 0.2, 0.25, 0.3, 0.35, 0.4, 0.45, 0.5, 0.55, 0.6, 0.65, 0.7, 0.75, 0.8$), where the best result is $TH_i = 0.65$ with red-boxed. (For interpretation of the references to color in this figure legend, the reader is referred to the web version of this article.)

GCE lacked effectiveness because the complex details affected the performance of the color-based ordering algorithm in color distinction. The mean shift clustering method shows outstanding performance in evaluating the NPRI and VoI, but was limited in terms of the segmented images in the subjective evaluation. Overall, the performance of CRC ordering was moderate, but it was more consistent with subjective human perception than the mean shift clustering method, especially in regions with small patches, and oversegmentation was rare. The objective evaluation of the proposed CRC ordering was not as accurate as that of the mean shift clustering method. Nevertheless, the resulting image obtained using the mean shift clustering method was inconsistent with human perceptual feelings, and the over-segmented conditions were globally reduced. In addition, we compared with the latest state-of-the-art segmentation methods such as segmentation by aggregating superpixels (SAS) [31] and SLIC superpixels [23], and the comparison results are shown in the second part of Table 1. Our proposed algorithm showed the best performance in evaluating the NPRI. However, in evaluating VoI, the GCE, and the BDE, it was the second-best method among all methods.

Figs. 3 and 4 show two test images used for comparing the three segmentation methods. The proposed CRC ordering method provides the most convincing segmentation results, with the segmentation boundary being visually close to the ground truth. However, the local threshold TH_i for the region merging algorithm is sensitive to the context of the test image. In short, different images require a specific threshold, such as 0.65 for the *airplane* image (see Fig. 3) and 0.5 for the *elephant* image (see Fig. 4).

4.3. Comparison of region merging algorithms

To analyze the dynamic properties of the segmentation algorithm when different merging thresholds were used for measuring the reliability of the system, the IQR was employed to describe the spread of the data for each evaluation index.

In Section 3.3, we mentioned that the quantitative-analysis-based region merging algorithm computed the HSI distance values between the reference colors of two neighboring regions. This method avoids the threshold determination problem of the CRC ordering method, and it uses the characteristics of the data cluster to select an appropriate threshold. We initially used the mean-shift-based image segmentation method to segment images, and the four indices were used to evaluate the results of the region merging algorithms. The proposed quartile-based method was also compared with the two other image segmentation methods.

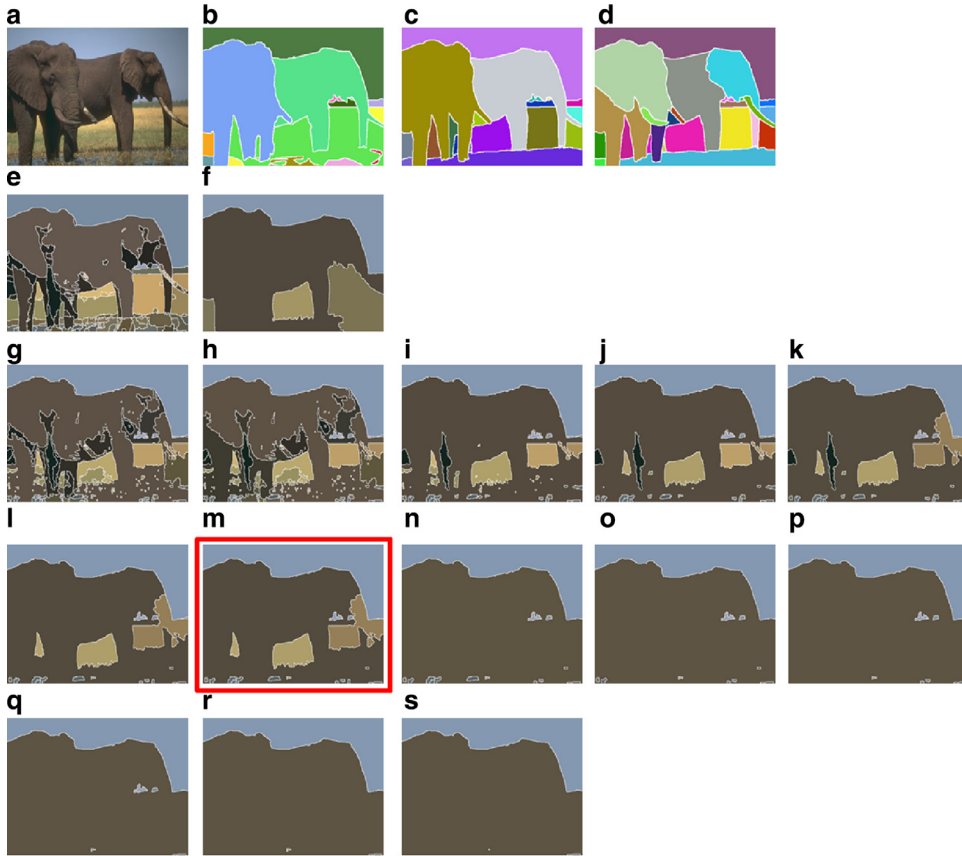


Fig. 4. Image segmentation results: elephants. (a) Original image, (b)–(d) ground-truth boundary, (e) mean-shift clustering method, (f) marker watershed method, (g)–(s) CRC-ordering result for different thresholds (i.e., $TH_t = 0.2, 0.25, 0.3, 0.35, 0.4, 0.45, 0.5, 0.55, 0.6, 0.65, 0.7, 0.75, 0.8$), where the best result is $TH_t = 0.5$ with red-boxed. (For interpretation of the references to color in this figure legend, the reader is referred to the web version of this article.)

Table 2
Comparison of different image segmentation algorithms.

Algorithms	Performance evaluations											
	NPRI [56]			Vol [37]			GCE [36]			BDE [20]		
	Rank1	Rank2	Rank3	Rank1	Rank2	Rank3	Rank1	Rank2	Rank3	Rank1	Rank2	Rank3
CRC-ordering	22 (7.3%)	94 (31.3%)	208 (69.3%)	96 (32.0%)	202 (67.3%)	281 (93.7%)	106 (35.3%)	200 (66.7%)	256 (85.3%)	23 (7.7%)	80 (26.7%)	214 (71.3%)
Quartile	38 (12.7%)	134 (44.7%)	224 (74.7%)	66 (22.0%)	147 (49.0%)	291 (97.0%)	69 (23.0%)	139 (46.3%)	211 (70.3%)	47 (15.7%)	195 (65.0%)	253 (84.3%)
Watershed-based [42]	11 (3.7%)	94 (31.3%)	183 (61.0%)	125 (41.7%)	216 (72.0%)	269 (89.7%)	111 (37.0%)	195 (65.0%)	238 (79.3%)	4 (1.3%)	34 (11.3%)	134 (44.7%)
Mean-shift [13]	229 (76.3%)	278 (92.7%)	284 (94.7%)	13 (4.3%)	35 (11.7%)	59 (19.7%)	14 (4.7%)	66 (22.0%)	195 (65.0%)	226 (75.3%)	291 (97.0%)	299 (99.7%)

In Table 2, we can observe that the accuracy of the NPRI and BDE indices increased by approximately 10% when the quartile method was employed. However, the accuracies of Vol and the GCE indices were below expectations. The overall performance of CRC ordering (with a hard threshold TH_t of 0.65) and the quartile method was more homogeneous than that of the other two methods. On average, the number of images with a Rank-2 score was over 150. The images in Fig. 5 show that the segmentation results of the quartile method were superior to those of the mean-shift-based and CRC ordering methods. Perceptually, the results of the mean shift clustering method were oversegmented, whereas the CRC ordering method was undersegmented. Compared with the ground truth images, the proposed quartile method yielded the robust segmentation results. Nevertheless, the evaluation with Vol and GCE indices lacked effectiveness because the quartile method avoided oversegmentation, resulting in a small region being ignored. In addition, we used only color information. It was difficult to differentiate between the foreground and the background when they had similar color tones. Fig. 6 shows the results of

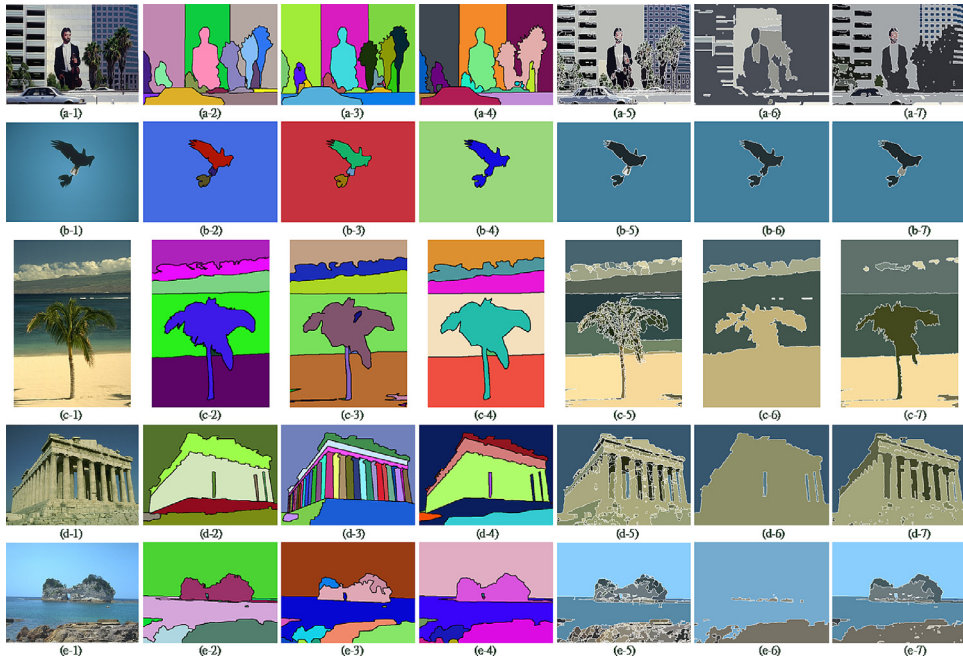


Fig. 5. Comparisons of automatic image segmentation. (1) Original image, (2)–(4) ground truth images, (5) mean-shift clustering method, (6) CRC-ordering method ($TH_1 = 0.65$), (7) based on quartile analysis.



Fig. 6. Examples of segmentation derived by the proposed algorithm on 30 images from the Berkeley Segmentation Database (Algorithm 2: quartile method).

the proposed image segmentation method and the corresponding scores of the indices when the quartile-based threshold determination method was used. Normally, we obtained comprehensive results with less small patches and isolated holes.

5. Conclusions

In this paper, we presented a color-based adaptive MM method involving a color-alone feature for dealing with the image segmentation problem. The similarity measure of the merging process between neighboring pixels and regions can be obtained as the solution of a ranking problem by using this method. In addition, we solved the threshold-sensitive problem by using the CRC ordering scheme for region merging. The HSI distance was measured for determining the rank of the color vectors and the likelihood of two adjacent regions being merged. Furthermore, the proposed CRC ordering scheme was applied together with the global reference color selection scheme for conducting color morphological processing. An alternative method involving a threshold determination step and based on quartile analysis was proposed for avoiding the CRC ordering method; the method was successfully verified.

Acknowledgment

This study was partially supported by the Ministry of Science and Technology, Taiwan, under Grants NSC 102-2221-E-155-037-MY2 and MOST 103-2221-E-155-027-MY2.

Reference

- [1] J. Angulo, J. Serra, Modeling and segmentation of colour images in polar representations, *Image Vis. Comput* 25 (4) (2007) 475–495.
- [2] J. Angulo, Morphological color processing based on distances. Application to color denoising and enhancement by centre and contrast operators, in: *Proceedings of the IASTED International Conference on Visualization, Imaging, and Image Processing (VIIP'2005)*, September 2005, pp. 314–319.
- [3] J. Angulo, Morphological colour operators in totally ordered lattices based on distances: Application to image filtering, enhancement and analysis, *Comput. Vis. Image Underst.* 107 (1–2) (2007) 56–73.
- [4] J. Angulo, Unified morphological colour processing framework in a lum/sat/hue representation, in: *Proceedings of the International Symposium on Mathematical Morphology (ISMM'05)*, 2005, pp. 387–396.
- [5] E. Aptoula, S. Lefèvre, C. Collet, Mathematical morphology applied to the segmentation and classification of galaxies in multispectral images, in: *Proceedings of the Fourteenth European Signal Processing Conference (EUSIPCO'06)*, 2006.
- [6] E. Aptoula, S. Lefèvre, A comparative study on multivariate mathematical morphology, *Pattern Recognit.* 40 (11) (2007) 2914–2929.
- [7] E. Aptoula, S. Lefèvre, Morphological description of color images for content-based image retrieval, *IEEE Trans. Image Process.* 18 (11) (2009) 2505–2517.
- [8] E. Aptoula, S. Lefèvre, On lexicographical ordering in multivariate mathematical morphology, *Pattern Recognit. Lett.* 29 (2) (2008) 109–118.
- [9] E. Aptoula, S. Lefèvre, On the morphological processing of hue, *Image Vis. Comput.* 27 (9) (2009) 1394–1401.
- [10] T. Athanasiadis, P. Mylonas, Y. Avrithis, S. Kollias, Semantic image segmentation and object labeling, *IEEE Trans. Circuits Syst. Video Technol.* 17 (3) (2007) 298–312.
- [11] Berkeley Segmentation Dataset Available online <<http://www.eecs.berkeley.edu/Research/Projects/CS/vision/bsds/>>, 2014 (accessed 22.01.14).
- [12] C.L.P. Chen, C.-Y. Zhang, Data-intensive applications, challenges, techniques and technologies: A Survey on Big Data, *Inf. Sci.* 275 (2014) 314–347.
- [13] D. Comaniciu, P. Meer, Mean shift: A robust approach toward feature space analysis, *IEEE Trans. Pattern Anal. Mach. Intell.* 24 (5) (2002) 603–619.
- [14] M.L. Comer, E.J. Delp, Morphological operations for colour image processing, *J. Electron. Imaging* 8 (3) (1999) 279–289.
- [15] Y. Deng, B.S. Manjunath, Unsupervised segmentation of color-texture regions in images and video, *IEEE Trans. Pattern Anal. Mach. Intell.* 23 (8) (2001) 800–810.
- [16] H. Deng, D.A. Clausi, Unsupervised image segmentation using a simple MRF model with a new implementation scheme, *Pattern Recognit.* 37 (12) (2004) 2323–2335.
- [17] M.C. d'Ornellas, J.A.T. Borges da Costa, Color mathematical morphology based on partial ordering of spectra, in: *Proceedings of the XX Brazilian Symposium on Computer Graphics and Image Processing (SIBGRAPI'07)*, 2007, pp. 37–44.
- [18] A.N. Evans, Nonlinear operations for colour images based on pairwise vector ordering, in: *Proceedings of the Digital Imaging Computing: Techniques and Applications (DICTA'05)*, 2005, p. 61.
- [19] P.F. Felzenszwalb, D.P. Huttenlocher, Efficient graph-based image segmentation, *Int. J. Comput. Vis.* 59 (2) (2004) 167–181.
- [20] J. Freixenet, X. Munoz, D. Raba, J. Martí, X. Cufí, Yet another survey on image segmentation: Region and boundary information integration, in: *Proceedings of the Seventh European Conference on Computer Vision Part III*, Copenhagen, Denmark, 2002, pp. 408–422.
- [21] P. Gonzalez, V. Cabezaz, M. Mora, F. Cordova, J. Vidal, Morphological color images processing using distance-based and lexicographic order operators, in: *Proceedings of the XXIX International Conference of the Chilean Computer Science Society (SCCC'10)*, 2010, pp. 258–264.
- [22] A.G. Hanbury, J. Serra, Morphological operators on the unit circle, *IEEE Trans. Image Process.* 10 (12) (2001) 1842–1850.
- [23] C.Y. Hsu, J.J. Ding, Efficient image segmentation algorithm using SLIC superpixels and boundary-focused region merging, in: *Proceedings of the Ninth Information, Communication and Signal Processing (ICICS)*, 2013, pp. 1–5.
- [24] R.J. Hyndman, Y. Fan, Sample quantiles in statistical packages, *Am. Stat.* 50 (1996) 361–365.
- [25] D.E. Ilea, P.F. Whelan, CTex—An adaptive unsupervised segmentation algorithm based on color-texture coherence, *IEEE Trans. Image Process.* 17 (10) (2008) 1926–1939.
- [26] D.E. Ilea, P.F. Whelan, Image segmentation based on the Integration of colour-texture descriptors – A review, *Pattern Recognit.* 44 (10) (2011) 2479–2501.
- [27] R. Kara-Falah, P. Bolon, J.P. Cocqueruz, A region-region and region-edge cooperative approach of image segmentation, in: *Proceedings of the IEEE International Conference on Image Processing, ICIP, 1994*, pp. 470–474.
- [28] M. Krinidis, I. Pitas, Color texture segmentation based on the modal energy of deformable surfaces, *IEEE Trans. Image Process.* 18 (7) (2009) 1613–1622.
- [29] O. Lezoray, A. Elmoataz, C. Meurie, Mathematical Morphology in any color space, in: *Proceedings of the IEEE Fourteenth International Conference on Image Analysis and Processing Workshops (ICIAPW'07)*, 2007, pp. 183–187.
- [30] H. Li, F. Meng, Q. Wu, B. Luo, Unsupervised multiclass region co-segmentation via ensemble clustering and energy minimization, *IEEE Trans. Circuits Syst. Video Technol.* 24 (5) (2014) 789–801.
- [31] Z. Li, X.M. Wu, S.F. Chang, Segmentation using superpixels: A bipartite graph partitioning approach, in: *Proceedings of the IEEE on Computer Vision and Pattern Recognition, CVPR, 2012*, pp. 789–796.
- [32] G. Louverdis, M.I. Vardavouli, I. Andreadis, Ph. Tsalides, A new approach to morphological color image processing, *Pattern Recognit.* 35 (8) (2002) 1733–1741.
- [33] R. Lukac, B. Smolka, K. Martin, K.N. Plataniotis, A.N. Venetsanopoulos, Vector filtering for color imaging, *IEEE Signal Process. Mag.* 22 (1) (2005) 74–86.

- [34] C. Lynch, Big data: how do your data grow? *Nature* 455 (7209) (2008) 28–29.
- [35] W.Y. Ma, B.S. Manjunath, EdgeFlow: A technique for boundary detection and image segmentation, *IEEE Trans. Image Process.* 9 (8) (2000) 1375–1388.
- [36] D. Martin, C. Fowlkes, D. Tal, J. Malik, A database of human segmented natural images and its application to evaluating segmentation algorithms and measuring ecological statistics, in: *Proceedings of Eighth International Conference on Computer Vision*, 2001, pp. 416–423.
- [37] M. Meila, Comparing clusterings-An axiomatic view, in: *Proceedings of the Twenty Second International Conference on Machine Learning*, 2005, pp. 577–584.
- [38] C. Meurie, O. Lezoray, L. Khoudour, A. Elmoataz, Morphological hierarchical segmentation and color spaces, *Int. J. Imaging Syst. Technol.* 20 (2) (2010) 167–178.
- [39] H. Min, W. Jia, X.F. Wang, Y. Zhao, R.X. Hu, Y.T. Luo, F. Xue, J.T. Lu, An intensity-texture model based level set method for image segmentation, *Pattern Recognit.* 48 (4) (2015) 1547–1562.
- [40] T.M. Nguyen, Q.M.J. Wu, Fast and robust spatially constrained Gaussian mixture model for image segmentation, *IEEE Trans. Circuits Syst. Video Technol.* 23 (4) (2013) 621–635.
- [41] R. Orduna, A. Jurio, D. Paternain, H. Bustince, P. Melo-Pinto, E. Barrenechea, Segmentation of color images using a linguistic 2-tuples model, *Inf. Sci.* 258 (2014) 339–352.
- [42] K. Parvati, B.S. Prakasa Rao, M. Mariya Das, Image segmentation using gray-scale morphology and marker-controlled watershed transformation, *Dyn. Nat. Soc.* 2008 (2008), Article ID 384346, 8 pages.
- [43] V. Patrascu, New fuzzy color clustering algorithm based on hsl similarity, in: *Proceedings of World Congress and 2009 European Society of Fuzzy Logic and Technology Conference*, 2009, pp. 48–52.
- [44] M. Pesaresi, J.A. Benediktsson, A new approach for the morphological segmentation of high-resolution satellite imagery, *IEEE Trans. Geosci. Remote Sens.* 39 (2001) 309–320.
- [45] T. Randen, J.H. Husoy, Filtering for texture classification: A comparative study, *IEEE Trans. Pattern Anal. Mach. Intell.* 21 (4) (1999) 291–310.
- [46] E. Saber, A. Tekalp, G. Bozdagi, Fusion of color and edge information for improved segmentation and edge linking, *Image Vis. Comput.* 15 (10) (1997) 769–780.
- [47] I. Santillan, I.R. Terol-Villalobos, G. Herrera-Ruiz, Color morphological image segmentation on a new opponent color space based on the notion of critical functions, in: *Proceedings of the Seventh Mexican International Conference on Artificial Intelligence (MICA'08)*, 2008, pp. 213–219.
- [48] O. Severino Jr, A. Gonzaga, A new approach for color image segmentation based on color mixture, *Mach. Vis. Appl.* 24 (3) (2013) 607–618.
- [49] J. Shen, Y. Du, X. Li, Interactive segmentation using constrained Laplacian optimization, *IEEE Trans. Circuits Syst. Video Technol.* 24 (7) (2014) 1088–1100.
- [50] J. Shi, J. Malik, Normalized cuts and image segmentation, *IEEE Trans. Pattern Anal. Mach. Intell.* 22 (8) (2000) 888–905.
- [51] H.C. Shih, An unsupervised hair segmentation and counting system in microscopy images, *IEEE Sens. J.* 15 (6) (2015) 3565–3572.
- [52] H.C. Shih, E.R. Liu, Adaptive region merging approach for morphological color image segmentation, in: *Proceedings of the ACCV Workshop on Feature and Similarity Learning for Computer Vision*, Singapore, 2014.
- [53] H.C. Shih, K.C. Yu, SPiRAL aggregation map (SPLAM): A new descriptor for robust template matching with fast algorithm, *Pattern Recognit.* 48 (5) (2015) 1707–1723.
- [54] L. Sun, T. Shibata, Unsupervised object extraction by contour delineation and texture discrimination based on oriented edge features, *IEEE Trans. Circuits Syst. Video Technol.* 24 (5) (2014) 780–788.
- [55] L.G. Ugarriza, E. Saber, S.R. Vantaram, V. Amuso, M. Shaw, R. Bhaskar, Automatic image segmentation by dynamic region growth and multiresolution merging, *IEEE Trans. Image Process.* 18 (10) (2009) 2275–2288.
- [56] R. Unnikrishnan, C. Pantofaru, M. Hebert, Toward objective evaluation of image segmentation algorithms, *IEEE Trans. Pattern Anal. Mach. Intell.* 28 (6) (2007) 929–944.
- [57] S. Velasco-Forero, J. Angulo, Supervised ordering in IRp: Application to morphological processing of hyperspectral images, *IEEE Trans. Image Process.* 20 (11) (2011) 3301–3308.
- [58] L. Vincent, P. Soille, Watersheds in digital spaces: An efficient algorithm based on immersion simulations, *IEEE Trans. Pattern Anal. Mach. Intell.* 13 (6) (1991) 583–598.
- [59] L. Wang, Y. Zhang, J. Feng, On the Euclidean distance of images, *IEEE Trans. Pattern Anal. Mach. Intell.* 27 (8) (2005) 1334–1339.
- [60] A.R. Weeks, L.J. Sartor, Color morphological operators using conditional and reduced ordering, in: *Proceedings of the SPIE Applications of Digital Image Processing XXII*, 1999.
- [61] J. Yang, J. Liu, J. Zhong, Anisotropic diffusion with morphological reconstruction and automatic seeded region growing for color image segmentation, in: *Proceedings of the International Symposium on Information Science and Engineering (ISISE'08)*, 2008, pp. 591–595.
- [62] S. Yang, Y. Lv, Y. Ren, L. Yang, L. Jiao, Unsupervised images segmentation via incremental dictionary learning based sparse representation, *Inf. Sci.* 269 (2014) 48–59.
- [63] C. Zhao, A new vectorial ordering for color morphology based on marginal ordering, in: *Proceedings of the Fifth International Conference on Computer Science and Education (ICCS'E'10)*, 2010, pp. 1769–1772.